Abdominal Imaging

Published online: 2 September 2009

Abdom Imaging (2010) 35:629–635
DOI: 10.1007/s00261-009-9569-9

In vivo identification of uric acid stones with dual-energy CT: diagnostic performance evaluation in patients

Paul Stolzmann,[1] Marko Kozomara,[2] Natalie Chuck,[1] Michael Müntener,[2] Sebastian Leschka,[1] Hans Scheffel,[1] Hatem Alkadhi[1]

[1]Institute of Diagnostic Radiology, University Hospital Zurich, Raemistr. 100, 8091 Zurich, Switzerland
[2]Department of Urology, University Hospital Zurich, Raemistr. 100, 8091 Zurich, Switzerland

Abstract

Background: To prospectively investigate the in vivo diagnostic performance of dual-energy (DE) computed tomography (CT) for the differentiation between uric acid (UA)-containing and non-UA-containing urinary stones.
Methods: DE CT scans were performed in 180 patients with suspected urinary stone disease using a dual-source CT scanner in the DE mode (tube voltages 80 and 140 kV). Urinary stones were classified as UA-containing or non-UA-containing based on CT number measurements and DE software results. Sensitivity, specificity, positive predictive values (PPV), and negative predictive values (NPV) for the detection of UA-containing urinary stones were calculated using the crystallographic stone analysis as the reference standard.
Results: DE CT detected 110/180 patients (61%) with urinary stone disease. In 53 patients, stones were sampled. Forty-four out of 53 stones (83%) were non-UA-containing; and nine stones (17%) were UA-containing. The software automatically mapped 52/53 (98%) stones. One non-UA-containing stone (UA, 2 mm) was missed; one UA-containing stone (3 mm) was misclassified by software analysis. The sensitivity, specificity, PPV, and NPV for the detection of UA-containing stones was 89% (8/9, 95% CI: 52–100%), 98% (43/44, 95% CI: 88–100%), 89% (8/9, 95% CI: 52–100%), and 98% (43/44, 95% CI: 88–100%).
Conclusion: Our results indicate that DE dual-source CT permits for the accurate in vivo differentiation between UA-containing and non-UA-containing urinary stones.

Correspondence to: Paul Stolzmann; *email:* paul.stolzmann@usz.ch

Key words: Dual energy—Computed tomography—Uric acid—Urinary stone—In vivo—Crystallography

Current evidence suggests an increasing prevalence of urinary stone disease in Western countries [1, 2]. The Urological Diseases in America project documented sharp increases in office visits, ambulatory procedures, and in-patient hospitalizations due to urinary lithiasis [1]. Main determinants in the clinical care of patients with urolithiasis are the location, size, and chemical composition of the calculi [3], the latter being particularly important in the presence of uric acid (UA) stones. Because UA stones may be dissolved by urinary alkalinization alone [4], external shock wave lithotripsy (ESWL) or interventional procedures such as ureteroscopy for stone removal could be sidestepped, thus avoiding the procedure-related complications in 3–6% of patients [5].

The imaging modality of choice for the detection of urinary stone disease is unenhanced computed tomography (CT), offering high specificity and sensitivity [6–8]. Earlier studies indicated that determining the stone composition by analyzing CT numbers at different X-ray energies is superior to analyzing with single energy CT [9, 10]. Despite promising in vitro results, however, the transferability of results to an in vivo setting was hampered by misregistration problems [11, 12]. More recently, urinary stone characterization by CT was revived using dual-source CT with dual-energy (DE) scans [13–19]. All of these studies, however, were performed in renal phantoms using ex vivo renal stones [13–19]. Only one study tested DE CT in vivo; however, this setting lacked crystallographic proof of the true stone composition [14].

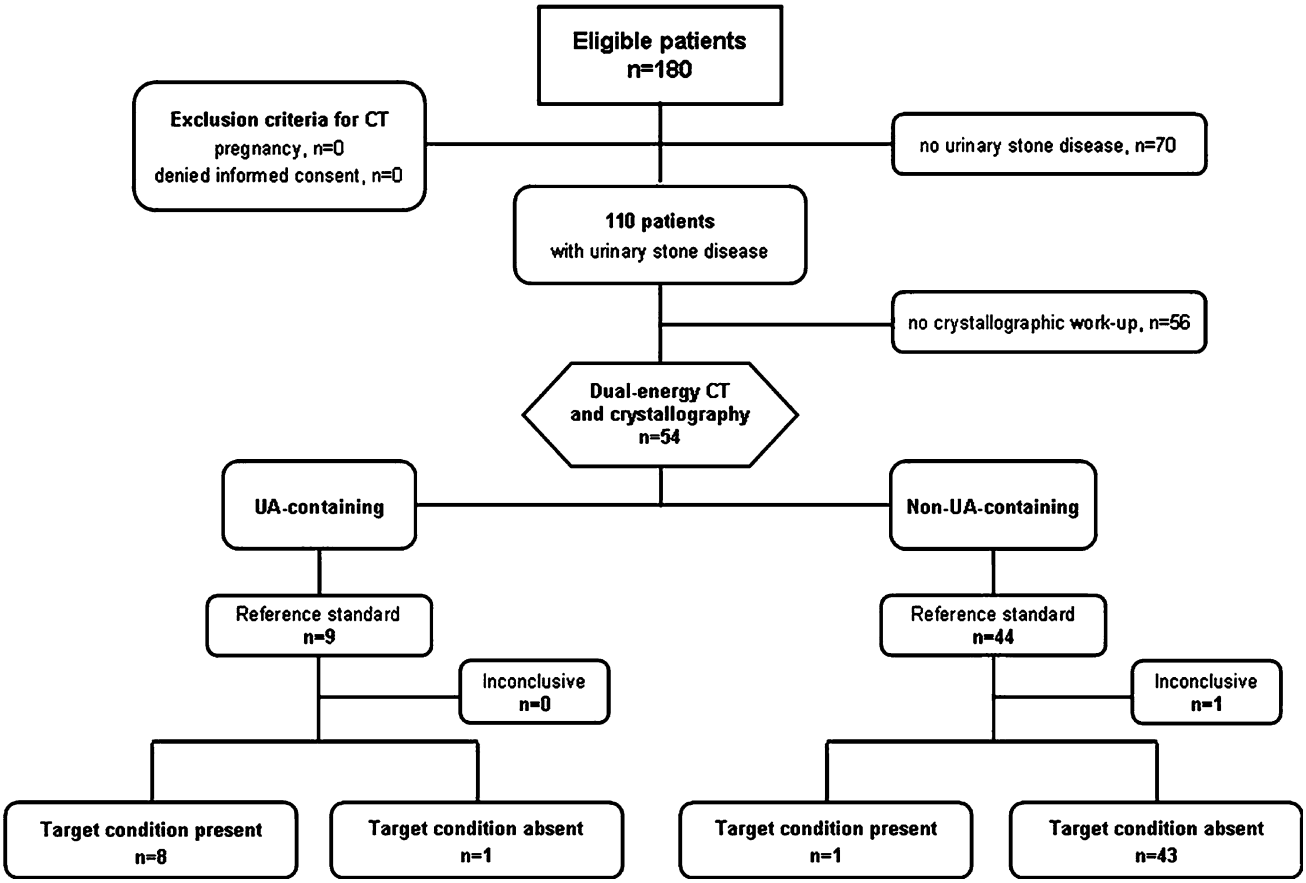

Fig. 1. Flow chart of the study. Target condition = urinary stone containing uric acid.

The aim of the present study was to prospectively evaluate the in vivo diagnostic performance of DE dual-source CT for differentiation between UA-containing and non-UA-containing urinary calculi using crystallography as the reference standard.

Methods

Patients

The study was approved by the ethics committee of our university, and written informed consent was obtained from all patients.

During an 8-month period, 180 consecutive patients (77 female patients, age 49 ± 14 years, range 29–87 years) with suspected urinary stone disease were prospectively enrolled. Pregnancy demonstrated the sole contraindication for non-enhanced CT ($n = 0$).

CT detected urinary stone disease in 110/180 patients (61%) (Fig. 1). Urinary stones or fragments were sampled in 54/110 patients (49%) by urinary straining ($n = 16$), ureteroscopy ($n = 14$), percutaneous nephrolitholapaxy ($n = 7$), or after ESWL ($n = 17$).

Data acquisition and reconstruction

All examinations were performed on a dual-source CT scanner (Definition, Siemens Medical Solutions, Forchheim, Germany) using a non-contrast enhanced protocol. CT data was acquired in the DE mode. Tube A and B were operated at 140 and 80 kV, and corresponding quality reference tube current time products were set at 90 and 350 mAs/rot, respectively. Corresponding detector sizes of tube A and B were 50 and 26 cm [20]. The following scanning parameters were used: slice collimation, $2 \times 32 \times 0.6$ mm^3; slice acquisition, $2 \times 64 \times 0.6$ mm^3 by use of a z-flying focal spot, gantry rotation time 330 ms, and pitch 0.70. Fully automated real-time anatomy based dose regulation (CAREDose4D, Siemens Medical Solutions, Forchheim, Germany) was used in all scans.

The 80 and 140 kV images were reconstructed with a slice thickness of 1.5 mm and a slice increment of 1.0 mm. For optimal DE post-processing dedicated convolution kernels are recommended, for this reason the kernel D20f was chosen for the DE scans. This results in a similar noise level to the B20f, but causes less overshoots at objects edges.

Additional reconstructions of weighted-average images from the raw spiral projection data of both tubes were performed. The attenuation in Hounsfield units (HU) on these weighted-average images was calculated during reconstruction with a composition ratio of 0.3 by using the following formula: $HU_{weighted\text{-}average} = 0.3 \times HU_{80\ kV} + 0.7 \times HU_{140\ kV}$. These images are as 120 kV images and allow for multi-planar and three-dimensional reconstructions [13–15, 18, 19, 21–23].

Data analysis

Image quality. Two blinded and independent readers (with 3 and 8 years of experience in abdominal radiology) assessed the interpretative quality of weighted-average images of each examination. Overall scan acceptability was assessed on a four-point scale as follows: 4 = inacceptable, 3 = marginally to fairly acceptable, 2 = acceptable, and 1 = very acceptable [24]. In addition, image noise (standard deviation (SD) of HU) was twice measured by a third radiologist at two levels on the psoas muscle (the mid kidney and the top of the iliac crests) [24] by carefully placing a region of interest (ROI), avoiding areas of inhomogeneity and muscle borders.

Urinary stone disease

For diagnosing or excluding urolithiasis, the same readers who evaluated the interpretative quality reviewed weighted-average images in an interactive mouse-driven cine mode. Both were asked to determine the presence or absence of uroliths and, if present, to ascribe uroliths to their location in the ureteral system (pelvicaliceal system, ureter, and bladder). The aforementioned four-point scale was used to determine the conspicuity and margins of each urinary stones on a per-patient basis. One of the readers was requested to document the size of each stone as measured with standard electronic calipers provided by the viewing software on the workstation. Size measurements (defined as the longest diameter from edge to edge) on weighted-average images were performed using bone window settings (center: 500 HU/width: 2000 HU).

Urinary stone analysis

The reconstructed 80 and 140 kV images were analyzed using commercially available DE software (''Kidney Stones'', Dual Energy Syngo, Software Version VA31, Siemens, Forchheim, Germany). We used a two-material decomposition described in detail elsewhere [13]. Urinary stones were considered to be a mixture of a hypothetical stone having no pores and the material occupying the pores (e.g., urine). The line between CT numbers at 80 and 140 kV of both urine and the pure stone data points characterized each urinary stones composition. The slope increments were then used to classify stones as whether or not they contained UA by applying a bisector line dividing the angle between UA and non-UA components.

The same readers who were asked to determine the presence or absence of uroliths and their location reviewed the color-coded software results and classified each urinary stone as containing UA or not. Both were blinded to the results from the other reader and from crystallographic analyses. Additionally, one reader was requested to measure the CT number [HU] of the urinary stones in each patient with standard metric software devices provided by the software. To determine the intra-observer variability of CT number measurements, ROI measurements (mean ROI area of 3.2 ± 1.6 mm^2, range 1–5 mm^2) were performed twice. DE indices (DEI) were calculated by the formula: $DEI = (HU_{80\ kV} - HU_{140\ kV})/(HU_{80\ kV} + HU_{140\ kV} + 2000)$ [14].

Crystallography

The composition of the urinary stones was determined by X-ray diffraction. The urinary stone sample was pulverized and analyzed by X-ray diffraction using a CubixPro diffractometer (PANalytical, Almelo, the Netherlands) using Ni-filtered Cu Kα radiation. The identification of the crystalline components was performed using the ICDD database and the semi-quantitative composition determined using the relative intensity of the different bands.

Statistical analysis

Results were expressed as absolute numbers, frequencies, medians, and means ± SD, if distributed normally. Inter-reader agreements were analyzed with kappa statistics: κ values of 0.00–0.20 were considered to indicate poor agreement; κ values of 0.21–0.40 fair agreement; κ values of 0.41–0.60 moderate agreement; κ values of 0.61–0.80 high agreement; and κ values of 0.81–1.00 excellent agreement.

The inter-observer variability concerning image noise and CT number measurements was assessed according to Bland and Altman and determined as the mean difference (bias) with adherent limits of agreement. Mean image noise values as well as mean CT numbers were compared using paired *t*-tests. DEIs of UA-containing and non-UA-containing urinary stones were compared using the unpaired Student's *t*-test. Receiver operating characteristic (ROC) analyses were fitted to DEI for the detection of UA. The area under the curve (AUC) with 95% confidence interval was calculated. A *P*-level of <0.05 was considered to indicate statistical significance.

The sensitivity, specificity, positive predictive values (PPV), and negative predictive values (NPV) were calculated from Chi-Square tests of contingency with crystallography as the reference standard. The 95%

confidence intervals (CI) were calculated from binomial expression. All statistical analyses were conducted using SPSS software (release 17.0, Chicago, IL, USA).

Results

Image quality

There was good inter-observer agreement ($k = 0.66$) in respect to the interpretative quality grading of weighted-average images. Image quality was considered as being of grade 1 and 2 (i.e., very acceptable and acceptable) in 52 patients (98.1%) by reader 1 and in 51/53 patients (96.2%) by reader 2. Agreement between both observers was achieved in 45/53 examinations (84.9%). Only one examination was rated as being of grade 3 (i.e., marginally to fairly acceptable) by both readers. None of the examinations was considered to be of grade 4 (i.e., not acceptable) by either reader.

Intra-observer variability concerning image noise measurements was small (mid kidney 0.1 HU, −1.1 to +1.2 HU; iliac crest, 0.0 HU, −1.4 to +1.3 HU). Mean image noise values were not significantly different (level of the mid kidney, $P = 0.42$; iliac crest, $P = 0.77$). Thus, means of measurements were taken for further analysis. Mean image at the level of the mid kidney was 12.05 ± 2.64 HU (6.60–17.40 HU) and was 11.37 ± 2.17 HU (7.05–16.55 HU) at the iliac crest, respectively.

Urinary stone disease

There was complete agreement between both readers ($k = 1.00$) regarding the diagnosis of urinary stone disease and stone location; therefore consensus reading was not required.

Weighted-average DE CT revealed 84 urinary stones (38 on the left, 44 on the right side, and 2 in the bladder) in the 53 patients (Table 1). Of these, 54/84 uroliths (62.3%) were located in the pelvicaliceal system in 39/53 patients (73.6%), whereas 28/84 uroliths (33.3%) were located in the ureter in 24/53 patients (45%).

Of the 28 uroliths, 4 (14.3%) were located in the proximal third, 5 (17.9%) were located in the middle third, and 19 (67.9%) were located in the distal third of the ureter. Two of the 84 total uroliths (2.4%) were located in the urinary bladder in 2/53 patients (3.7%). Thirty-three of the 53 patients (63.3%) had one urinary stone, and 20/53 patients (37.7%) had more than one urinary stone.

Table 1. Number of urinary stones detected and size measured with dual-energy CT

	Unenhanced CT
Uroliths/patients	84/53
Pelvicaliceal system	54/39
Ureter	28/24
Bladder	2/2
Mean stone size ± SD (range)	8.0 ± 7.1 mm (2–33 mm)

There was good interobserver agreement ($k = 0.64$) regarding the conspicuity and margins of each stone on weighted-average images of each examination. Conspicuity and margins were considered as being acceptably delineated (i.e., grade 1 and 2) in all 53 patients (100.0%) by both readers. Agreement between both observers was achieved in 46/53 examinations (86.8%).

The size of the 84 urinary stones on weighted-average images ranged between 1–12 mm (median 3.5 mm).

Urinary stone analysis

There was complete agreement between both readers ($k = 1.00$) concerning the classification as to whether or not the stones contained UA. Thus, consensus reading was not required. CT numbers showed an inter-observer variability of 0.5 HU (−45.5 to +46.5 HU) at 140 kV and of −1.1 HU (−49.9 to +47.7 HU) at 80 kV. Mean CT numbers did not significantly differ (140 kV, $P = 0.89$; 80 kV, $P = 0.76$). Thus, means of measurements were taken for further analysis.

The generation of dual-energy software results took 2 h 32 min in average. In the 20 patients with more than one stone, DE CT demonstrated no differences in composition of the stones (i.e., UA-containing vs. non-UA-containing) and CT numbers ($P = 0.53$). Thus, stone differentiation was performed on a per-patient basis. The DE analysis software automatically mapped 52/53 stones (98.1%). Based on the software results, both readers classified urinary stones in 8/53 patients (15.1%) as containing UA (Fig. 2A), while 44/53 (83.0%) were classified as non-UA-containing (Fig. 2B). One urinary stone (UA, 2 mm) in a patient with a single urinary stone was missed by software analysis and was not encoded in terms of color overlay. This stone was judged to contain UA in concordance with the intention to diagnose basis of this study—summing up to 9/53 patients (17.0%) with UA-containing urinary stones Mean CT numbers of UA-containing urinary stones were 251.6 ± 226.6 HU (108.1–736.7 HU) at 140 kV and 301.9 ± 198.5 HU (111.8–709.3 HU) at 80 kV. Non-UA-containing uroliths had a mean CT number of 546.1 ± 329.7 HU (162.2–1218.2 HU) at 140 kV and of 823.7 ± 507.6 HU (202.3–1920.0 HU) at 80 kV. These numbers resulted in corresponding mean DEI of 0.021 ± 0.018 and 0.075 ± 0.34, respectively, with a significantly ($P < 0.001$) lower mean DEI for UA-containing urinary stones.

Crystallography

The time interval between CT and stone analyses was less than 14 days in all patients (median 6 days, range 1–14 days). All 54 urinary stone samples obtained by urinary straining, surgical, and endoscopic interventions in

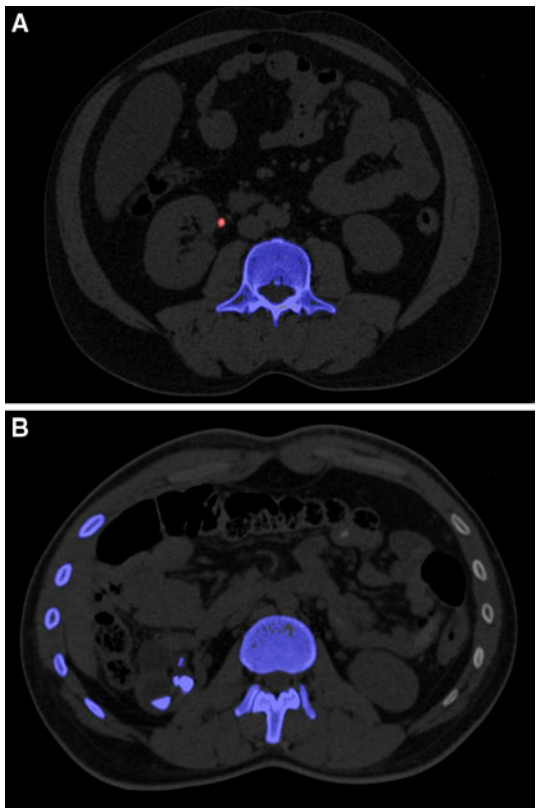

Fig. 2. **A** 47-year-old female patient suffering from right-sided acute flank pain. Weighted-average CT image with color-coded overlay demonstrates a 3-mm urinary stone in the proximal ureter and the composition of the stones. *Red* color indicates that the calculus consists of uric acid, confirmed by crystallography. Calcified structures of the adjacent vertebral body (i.e., apatite) are encoded in *blue*. **B** 35-year-old male patient with recurrent urolithiasis. Weighted-average CT image reveals three urinary stones (2, 4, and 8 mm) in the pelvicaliceal system. Crystallography confirmed CT results showing non-uric acid containing calculi (*blue* color overlay). Chemical analysis yielded 80% whewellite and 20% wheddellite for the surgically obtained stone specimens.

54 patients were transferred to clinical chemistry. In 1/54 patients (1.8%) stone sampling was insufficient to allow crystallographic analysis. Thus, the diagnostic performance is reported in 53 patients (20 female patients, 48 ± 14 years, range 30–80 years, body mass index 25.0 ± 3.3 kg/m^2, range 18.8–32.8 kg/m^2) who were included in the present study (Fig. 1).

The 53 urinary stone samples analyzed consisted of 13 different compositions (Table 2). Twenty-four urinary stone samples consisted of 6 pure compositions, while 29 consisted of seven different mixed compositions. X-ray diffraction revealed a total of 9/53 stone samples (17.0%) that contained UA and 44/53 (83%) that contained no UA, respectively.

The results of DE CT analyses were in agreement with crystallographic analyses in 51/53 patients (96%). One false-negative rating occurred in a patient with one ureteral stone being 3 mm in size using the software. This stone was proven to be mixed and composed of wheddellite/urate (80%/20%). The unmapped stone (2 mm) was composed of wheddellite/apatite (80%/20%) causing one false-positive rating due to considering the stone as containing UA.

Thus, the sensitivity of DE CT for the classification of urinary stones as containing UA was 88.9%, the specificity was 97.7%, the PPV was 88.9%, and the NPV was 97.7%, yielding a diagnostic accuracy of 96.0% (Table 3). When plotting the DEIs against the presence of UA, the ROC analyses revealed an AUC of 0.87 (95% CI: 73.1–95.4%, $P < 0.001$) with a best threshold of 0.04 for predicting UA-containing urinary stones (Fig. 3). The application of this threshold is associated with a sensitivity of 74.2% (95% CI: 55.4–88.1%) and in a specificity of 91.9% (95% CI: 58.7–98.5%).

Discussion

The present study is the first study to demonstrate that DE dual-source CT allows accurate in vivo differentiation between UA-containing and non-UA-containing urinary calculi. The sensitivity, specificity, PPV, and NPV of DE dual-source CT for the classification of urinary stones as containing UA were 88.9%, 97.7%, 88.9%, and 97.7%, respectively, yielding a diagnostic accuracy of 96.0%.

We also demonstrated that weighted-average DE CT can be utilized for both diagnostic imaging of the urinary tract and the diagnosis of urinary stone disease with high inter-observer agreements. This is in line with a study by Graser and coworkers [14]. In their study, all urinary calculi were clearly visible at all energy levels. Their results also showed that the weighted-average images derived from the DE CT acquisition compare well to single-energy 120 kV images.

Previous studies using two consecutive scans at two different energy levels with single-source CT had shown the feasibility of differentiating urinary calculi in vitro [9, 10]. In vivo, however, Grosjean et al. [11] showed that an overlap between different types of renal stones prohibited a reliable determination of the chemical composition by two subsequent scans. This was explained by movement of the kidneys as a result of respiration.

The problem of misregistration was solved by the introduction of dual-source CT which enables the simultaneous acquisitions of two X-ray spectra [20]. Although several studies demonstrated high accuracy for predicting urinary stones compositions in vitro [13–15, 19], studies have not yet evaluated the accuracy of DE CT in an in vivo setting.

Our study demonstrates in patients that the DE dual-source CT approach can accurately discriminate between UA and other stone types. The observed sensitivity and specificity were 89% and 98%, which are similar to those

Table 2. Compositions of pure and mixed urinary stones, maximum transverse diameters, and mixing ratios

Components[a]	Number	Sizes (mm)[b]	Mixing ratios (%)[a]
Pure stones			
Calcium oxalate	14	1–12	
Calcium phosphate	2	3, 4	
Uric acid	4	2–9	
Uric acid dihydrate	1	5	
Cystine	2	6, 7	
Ammonium magnesium phosphate (Struvite)	1	3	
Mixed stones			
Whewellite/wheddellite	11	1–10	90/10–10/90
Whewellite/apatite	3	4, 2, 5	80/20, 30/70, 10/90
Wheddellite/apatite	4	2–6	90/10–20/80
Whewellite/brushite	7	2–8	80/20
Uric acid/uric acid dihydrate	2	3, 4	90/10, 50/50
Wheddellite/urate	1	3	80/20
Hydrogen phosphate/acatanavir	1	3	30/70

[a] As determined by crystallography, [b] as determined on weighted-average CT images
Note: Urinary stone sizes and mixing ratios are given as range if more than three stones were present in the entire cohort

Table 3. In vivo diagnostic performance of dual-energy dual-source CT for the differentiation between UA-containing and non-UA-containing urinary stones

	n/n	Value (%)	95% CI (%)
Sensitivity	8/9	88.9	51.8–99.7
Specificity	43/44	97.7	88.0–100.0
Positive predictive value	8/9	88.9	51.8–99.7
Negative predictive value	43/44	97.7	88.0–100.0
Accuracy	51/53	96.2	87.0–99.5

CI confidence interval
Note: Diagnostic accuracy is based on software analysis results. Non-detected uroliths were classified as containing UA

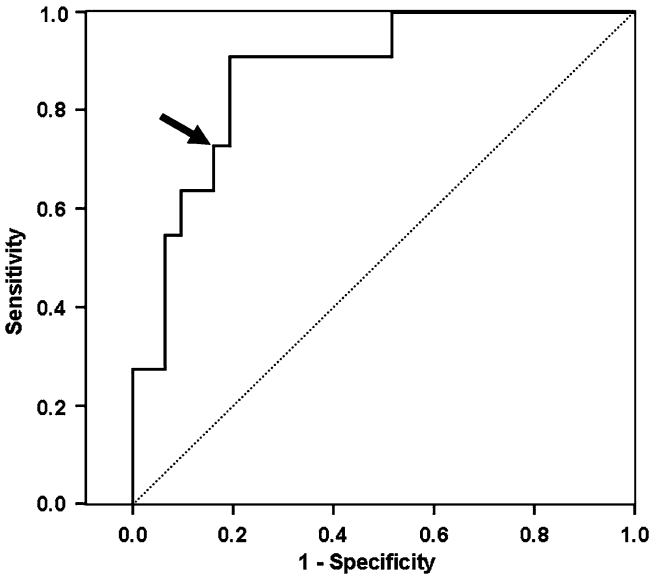

Fig. 3. The ROC curve for dual-energy indices of CT numbers at 80 and 140 kV adjusted for the presence of uric acid as evidenced by X-ray diffraction as reference standard. Best cut-off for the prediction of uric acid was found at a DEI of 0.04 (*arrow*), resulting in a 74.2% sensitivity and 91.9% specificity.

of DE ex vivo studies [13–15, 19]. One urinary stone (non-UA-containing, 2 mm) in one patient was missed by software analysis. One false-negative rating occurred in a mixed stone (3 mm) primarily composed of wheddellite (80%) with small amounts of UA (20%). Although not clinically relevant because of the high calcified partition hindering conservative treatment, this finding might be due to the reduced accuracy of DE CT for stones of approximately 3 mm in size or less, as previously evidenced in vitro [13].

When considering DEI for the differentiation of UA-containing urinary stones from other stone types [14], sensitivity and specificity were reduced to 74% and 91% in our study. This may be best explained by the nature of manual measurements which are strongly affected by the partial volume artifact [3]. Because urinary stones are porous and are considered as a mixture of a hypothetical pure stone with no pores and urine that fills the pores, CT numbers of voxels at the periphery of the stone are different from those in the center. The DE material decomposition algorithm used with dual-source CT is less affected by the partial volume error [13]. Considering the individual slope increment between CT numbers at 80 and 140 kV of both urine and the pure stones as the main determinants for stone characterization, each single

urinary stone voxel can be accurately characterized. Thus, partial volume averaging does not play such a significant role as it does in stone characterization based solely on CT number measurements. This was also proven in vitro by Boll et al. [16]. They showed that DE CT with advanced post-processing techniques improved the characterization of renal stone composition beyond that achieved with single-energy CT acquisitions and basic attenuation assessment [16].

The ability to predict the stone composition before treatment by CT helps in triaging patients. It enables the selection of patients with small UA-containing stones who benefit from medical management rather than shock wave lithotripsy [9, 10, 25]. In addition, DE CT may also impact on the management of patients with large UA stones which are treated by urinary alkalization in combination with prior fragmentation by extracorporeal shockwave lithotripsy considered as the reference management [4, 26, 27].

Limitation

Only a small number of mixed urinary stones (i.e., composed of both UA-containing and non-UA-containing partitions) were examined. Due to the limited number of stones, no distinction was made between pure and polycrystalline uric acid-, struvite-, cystine-, calcium oxalate, and calcium phosphate-, and brushite as recently shown possible in an anthropomorphic DE renal phantom study [16]. Some patients had several urinary calculi. Therefore, it remains uncertain which calculus was brought to analysis; however, no differences in stone compositions were noted within each patient with more than one stone. Finally, the study design did not allow an evaluation of how the a priori identification of UA in urinary calculi might have impacted on the clinical management of the patients.

Conclusion

Our in vivo results indicate that the differentiation between UA-containing and non-UA-containing stones can be accurately performed using DE dual-source CT.

Acknowledgments. This research was supported by the National Center of Competence in Research, Computer Aided and Image Guided Medical Interventions of the Swiss National Science Foundation.

References

1. Pearle MS, Calhoun EA, Curhan GC (2005) Urologic diseases in America project: urolithiasis. J Urol 173:848–857
2. Stamatelou KK, Francis ME, Jones CA, et al. (2003) Time trends in reported prevalence of kidney stones in the United States: 1976–1994. Kidney Int 63:1817–1823
3. Saw KC, McAteer JA, Monga AG, et al. (2000) Helical CT of urinary calculi: effect of stone composition, stone size, and scan collimation. AJR Am J Roentgenol 175:329–332
4. Coe FL, Evan A, Worcester E (2005) Kidney stone disease. J Clin Invest 115:2598–2608
5. Lindqvist K, Holmberg G, Peeker R, et al. (2006) Extracorporeal shock-wave lithotripsy or ureteroscopy as primary treatment for ureteric stones: a retrospective study comparing two different treatment strategies. Scand J Urol Nephrol 40:113–118
6. Yilmaz S, Sindel T, Arslan G, et al. (1998) Renal colic: comparison of spiral CT, US and IVU in the detection of ureteral calculi. Eur Radiol 8:212–217
7. Dalrymple NC, Verga M, Anderson KR, et al. (1998) The value of unenhanced helical computerized tomography in the management of acute flank pain. J Urol 159:735–740
8. Boulay I, Holtz P, Foley WD, et al. (1999) Ureteral calculi: diagnostic efficacy of helical CT and implications for treatment of patients. AJR Am J Roentgenol 172:1485–1490
9. Mostafavi MR, Ernst RD, Saltzman B (1998) Accurate determination of chemical composition of urinary calculi by spiral computerized tomography. J Urol 159:673–675
10. Deveci S, Coskun M, Tekin MI, et al. (2004) Spiral computed tomography: role in determination of chemical compositions of pure and mixed urinary stones—an in vitro study. Urology 64:237–240
11. Grosjean R, Sauer B, Guerra RM, et al. (2008) Characterization of human renal stones with MDCT: advantage of dual energy and limitations due to respiratory motion. AJR Am J Roentgenol 190:720–728
12. Johnson TR, Krauss B, Sedlmair M, et al. (2007) Material differentiation by dual energy CT: initial experience. Eur Radiol 17:1510–1517
13. Primak AN, Fletcher JG, Vrtiska TJ, et al. (2007) Noninvasive differentiation of uric acid versus non-uric acid kidney stones using dual-energy CT. Acad Radiol 14:1441–1447
14. Graser A, Johnson TR, Bader M, et al. (2008) Dual energy CT characterization of urinary calculi: initial in vitro and clinical experience. Invest Radiol 43:112–119
15. Stolzmann P, Scheffel H, Rentsch K, et al. (2008) Dual-energy computed tomography for the differentiation of uric acid stones: ex vivo performance evaluation. Urol Res 36:133–138
16. Boll DT, Patil NA, Paulson EK, et al. (2009) Renal stone assessment with dual-energy multidetector CT and advanced postprocessing techniques: improved characterization of renal stone composition—pilot study. Radiology 250:813–820
17. Fletcher JG, Takahashi N, Hartman R, et al. (2009) Dual-energy and dual-source CT: is there a role in the abdomen and pelvis? Radiol Clin North Am 47:41–57
18. Scheffel H, Stolzmann P, Frauenfelder T, et al. (2007) Dual-energy contrast-enhanced computed tomography for the detection of urinary stone disease. Invest Radiol 42:823–829
19. Matlaga BR, Kawamoto S, Fishman E (2008) Dual source computed tomography: a novel technique to determine stone composition. Urology 72:1164–1168
20. Flohr TG, McCollough CH, Bruder H, et al. (2006) First performance evaluation of a dual-source CT (DSCT) system. Eur Radiol 16:256–268
21. Boll DT, Merkle EM, Paulson EK, et al. (2008) Calcified vascular plaque specimens: assessment with cardiac dual-energy multidetector CT in anthropomorphically moving heart phantom. Radiology 249:119–126
22. Stolzmann P, Frauenfelder T, Pfammatter T, et al. (2008) Endoleaks after endovascular abdominal aortic aneurysm repair: detection with dual-energy dual-source CT. Radiology 249:682–691
23. Takahashi N, Hartman RP, Vrtiska TJ, et al. (2008) Dual-energy CT iodine-subtraction virtual unenhanced technique to detect urinary stones in an iodine-filled collecting system: a phantom study. AJR Am J Roentgenol 190:1169–1173
24. Paulson EK, Weaver C, Ho LM, et al. (2008) Conventional and reduced radiation dose of 16-MDCT for detection of nephrolithiasis and ureterolithiasis. AJR Am J Roentgenol 190:151–157
25. Williams JCJr, Saw KC, Paterson RF, et al. (2003) Variability of renal stone fragility in shock wave lithotripsy. Urology 61:1092–1096 (discussion 1097)
26. Ngo TC, Assimos DG (2007) Uric acid nephrolithiasis: recent progress and future directions. Rev Urol 9:17–27
27. Liebman SE, Taylor JG, Bushinsky DA (2007) Uric acid nephrolithiasis. Curr Rheumatol Rep 9:251–257